

# Temperature effect on green-synthesized $\text{Co}_3\text{O}_4$ nanoparticle as photocatalyst for overall water splitting

Qing-Yun Chen,<sup>a,\*</sup> Sajjad U. Haq,<sup>a</sup> Zhong-Hang Xing,<sup>a</sup>  
and Yun-Hai Wang<sup>b</sup>

<sup>a</sup>Xi'an Jiaotong University, International Research Center for Renewable Energy,  
State Key Laboratory of Multiphase Flow in Power Engineering, Xi'an, China

<sup>b</sup>Xi'an Jiaotong University, Department of Environmental Science and Engineering,  
Xi'an, China

**Abstract.**  $\text{Co}_3\text{O}_4$  nanoparticles were synthesized by a green synthesis method using bread fungus and cobalt nitrate hexahydrate as the precursors. The effects of the calcination temperature on the structure and properties of nanoparticles, and the ambient temperature on the photocatalytic reaction are discussed. The cubic structure of  $\text{Co}_3\text{O}_4$  nanoparticles was obtained, and the grain size was between 14 and 19 nm at different calcination temperatures.  $\text{Co}_3\text{O}_4$  calcined at 500°C shows good photocatalytic performance. Without adding any sacrificial agent and co-catalyst, the amount of hydrogen and oxygen released in 5 h were 259.4 and 135.7  $\mu\text{molg}^{-1}$ , respectively. The results show that, with the increase of ambient temperature, the evolution rate of hydrogen and oxygen is accelerated, and the atomic ratio of hydrogen to oxygen is close to 2:1. In addition, the  $\text{Co}_3\text{O}_4$  photocatalyst has good stability. Our study provides an environmentally friendly, low-cost, and efficient method for the preparation of cobalt oxide photocatalysts with excellent performance. © 2020 Society of Photo-Optical Instrumentation Engineers (SPIE) [DOI: [10.1117/1.JPE.10.042006](https://doi.org/10.1117/1.JPE.10.042006)]

**Keywords:** cobalt oxide; overall water splitting; green synthesis; hydrogen; oxygen.

Paper 20064SS received Aug. 5, 2020; accepted for publication Oct. 23, 2020; published online Nov. 3, 2020.

## 1 Introduction

With the serious energy crisis and increasing environmental concerns, development of better energy storage materials is urgently needed.<sup>1,2</sup> Photocatalytic water splitting is an environmentally friendly and promising way to store unexploited solar energy in the form of hydrogen because of its high energy density.<sup>3-5</sup> The photocatalyst is one of the key factors in the photocatalytic water splitting.<sup>6-9</sup> The major challenge in this area is to create a sustainable and efficient photocatalyst that can work well with visible light, which is the major component (i.e., ~50%) of the solar spectrum.<sup>10</sup> Nanostructured metal oxides (such as  $\text{TiO}_2$ ,  $\text{SnO}_2$ ,  $\text{Co}_3\text{O}_4$ ,  $\text{Fe}_2\text{O}_3$ ,  $\text{CuO}$ , and  $\text{WO}_3$ ) are novel materials for photocatalytic water splitting under visible light irradiation.<sup>11-15</sup> Among them,  $\text{Co}_3\text{O}_4$  as a p-type semiconductor is particularly attractive in this area because of its suitable bandgap of 3.95 to 2.13 eV.<sup>16</sup>

Synthesis of  $\text{Co}_3\text{O}_4$  nanoparticles has been reported using various methods, such as thermal decomposition,<sup>17</sup> template method,<sup>18</sup> hydrothermal method,<sup>19</sup> microwave-assisted,<sup>20</sup> and chemical spray pyrolysis.<sup>21</sup> These methods usually consume more energy, are capital intensive, and use toxic chemicals in the preparation process.<sup>16,22</sup> As an alternative to these traditional methods, green synthesis is considered to be a safe, economic, and ecological method for the preparation of nanoparticles.<sup>23</sup> Green synthesis by naturally derived materials, including plant extract and components and microorganisms, has been studied for mass production to detoxify and degrade hazardous pollutants.<sup>24,25</sup> For example, Abukhadra et al.<sup>26</sup> reported MCM-41/ $\text{Co}_3\text{O}_4$  nanocomposite was synthesized from rice husk silica gel and peach leaves, for enhanced photocatalytic degradation of acephate pesticide. Salam et al.<sup>27</sup> prepared organo-bentonite/ $\text{Co}_3\text{O}_4$  green

\*Address all correspondence to Qing-Yun Chen, [qychen@xjtu.edu.cn](mailto:qychen@xjtu.edu.cn)

nanocomposite and investigated it as a potential eco-friendly, low-cost adsorbent and photocatalyst for promising removal of both malachite green dye and Cr(VI) ions.

Therefore, developing an efficient and stable photocatalyst by an environmentally friendly, low-cost, and efficient green-synthesis method to accomplish the overall water splitting without using sacrificial agents, noble metals, and external bias is still a challenge. In this paper, we report on the green synthesis, characterization, and catalytic effect of the green-synthesized  $\text{Co}_3\text{O}_4$  nanoparticles on overall water splitting. The effects of the calcination temperature on the structure and properties, and the ambient temperature on the photocatalytic process, have also been reported.

## 2 Experimental

### 2.1 Green Synthesis of $\text{Co}_3\text{O}_4$ Nanoparticles

All reagents were of analytical reagent grade and used as received from Sinopharm Chemical Reagent Co., Ltd.  $\text{Co}_3\text{O}_4$  nanoparticles were synthesized using bread fungus as a green material. Initially, fungus was grown on bread by putting it in dark for more than 10 days. Cobalt nitrate [ $\text{Co}(\text{NO}_3)_2 \cdot 6\text{H}_2\text{O}$ ] was put into distilled water to form a 0.2 M reddish solution. Then fungus from bread was added until the red solution turned green. The green mixture was stirred for 3 h and kept the temperature at 50°C. After stirring for 3 h, the mixture was left in the dark overnight. The resulting mixture is then filtered, and the filtered solution was stored in an oven at 70°C to obtain a dark red, jelly-like mixture, which was calcined in a muffle furnace at different temperatures.

### 2.2 Characterization

The morphology of the  $\text{Co}_3\text{O}_4$  nanoparticles was determined via scanning electron microscopy (SEM) (JEOL JSM-7800F). X-ray diffraction (XRD) patterns were obtained from a PANalytical X'pert Pro MPD diffractometer operated at 40 kV and 40 mA using Ni-filtered  $\text{Cu K}\alpha$  irradiation ( $\lambda = 1.5406 \text{ \AA}$ ). A FEI Tecnai G2 F30 transmission electron microscope (TEM) was used to characterize the structure of  $\text{Co}_3\text{O}_4$  nanoparticles. UV-Vis absorption spectra were measured on a Hitachi U-4100 instrument equipped with a diffuse reflectance accessory.

### 2.3 Photocatalytic Reaction

The photocatalytic overall water splitting was carried out under visible light irradiation by using 300-W Xe lamp equipped with a 420-nm cutoff filter. 10 mg of  $\text{Co}_3\text{O}_4$  nanoparticles was added into 80 ml of water in a Pyrex cell with a side window for external-light incidence. The evolved gas was analyzed on a gas chromatograph (thermal conductivity detector, TDX-01 column,  $\text{N}_2$  as carrier gas) every 60 min.  $\text{N}_2$  was bubbled into the cell for 15 min before the photocatalytic reaction to remove  $\text{O}_2$ . The different ambient temperature for photocatalytic reaction was kept by thermostatic water bath.

## 3 Results and Discussion

To investigate the morphology of  $\text{Co}_3\text{O}_4$  nanoparticles, SEM was employed, and the results are shown in Fig. 1. As shown in Fig. 1(a), the nanoparticles calcined at 700°C show the hexagonal structure, some of which are very large in size. As can be seen from Figs. 1(b)–1(d), the nanoparticles calcined at 600°C, 500°C, and 400°C have spherical structure, and the distribution is very uniform. On the other hand, the nanoparticles calcined at 400°C are very large and agglomerated as shown in Fig. 1(e), which are not suitable for use as photocatalysts.

Figure 2 presents the XRD pattern of  $\text{Co}_3\text{O}_4$  nanoparticles calcined at different temperatures. The peaks at  $2\theta$  values [19.1 deg, 31.2 deg, 36.9 deg, 38.5 deg, 44.8 deg, 55.6 deg, 59.4 deg, 65.3 deg, 74.1 deg, and 77.3 deg corresponding to (111), (200), (311), (222), (400), (422), (511),

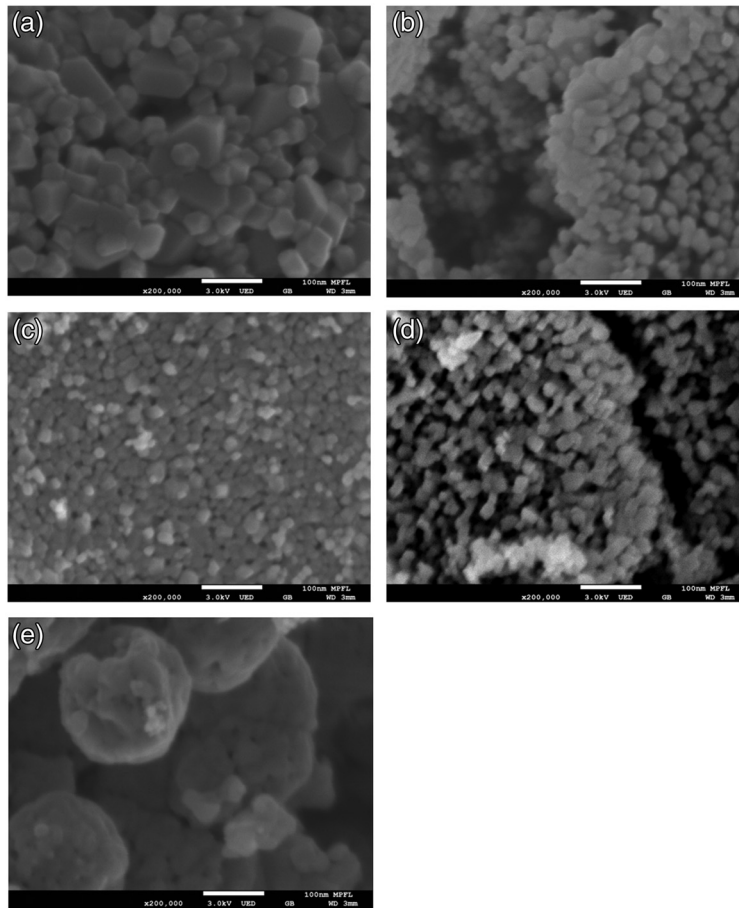


**Fig. 1** SEM images of  $\text{Co}_3\text{O}_4$  nanoparticles calcined at the different temperature: (a)  $700^\circ\text{C}$ , (b)  $600^\circ\text{C}$ , (c)  $500^\circ\text{C}$ , (d)  $450^\circ\text{C}$ , and (e)  $400^\circ\text{C}$ .

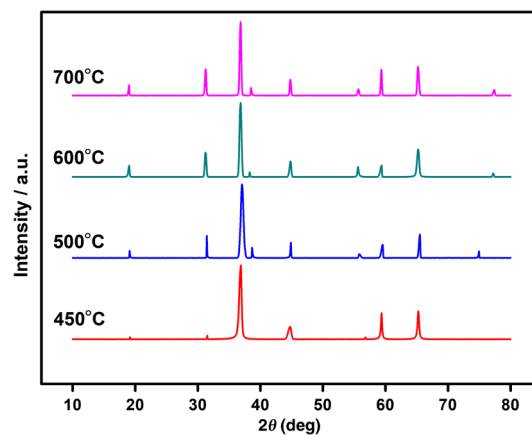


**Fig. 2** XRD spectrum of  $\text{Co}_3\text{O}_4$  calcined at different temperatures.

(440), (620), and (533) planes of  $\text{Co}_3\text{O}_4$ , respectively] are indexed to the cubic  $\text{Co}_3\text{O}_4$  (JCPDS42-1467).<sup>28,29</sup> It can be seen from Fig. 2, there is no other impurity peak, indicating high purity of  $\text{Co}_3\text{O}_4$ . At the same time, the diffraction peak is sharp, suggesting that the crystallinity of  $\text{Co}_3\text{O}_4$  is relatively high. But with the increase in temperature, the small peaks according to (222), (422), (620), or (533) planes of  $\text{Co}_3\text{O}_4$  appeared, which may be due to the morphology of  $\text{Co}_3\text{O}_4$  as shown in Fig. 1. By using Sheerer formula  $D = 0.94\lambda/\beta \cos \theta$ , the

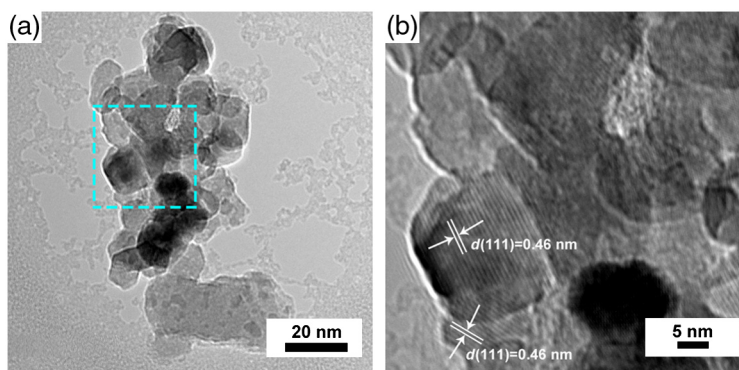


**Fig. 3** TEM images of  $\text{Co}_3\text{O}_4$  nanoparticles calcined at  $500^\circ\text{C}$ : (a) low magnification and (b) high magnification.

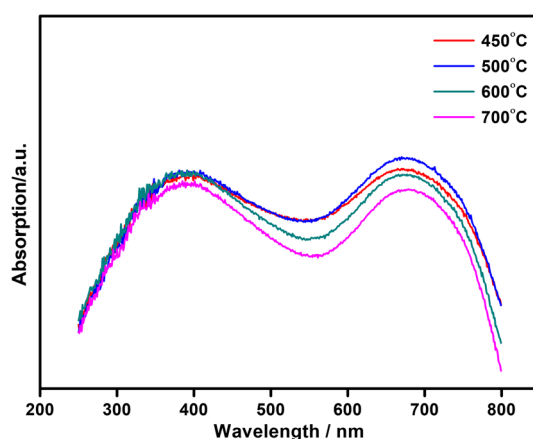


**Fig. 4** UV-Vis spectrum of  $\text{Co}_3\text{O}_4$  calcined at different temperatures.

size of  $\text{Co}_3\text{O}_4$  nanoparticles according to the diffraction peak of (311) crystal plane is 15, 14, 19, and 18 nm for the calcination temperature at  $450^\circ\text{C}$ ,  $500^\circ\text{C}$ ,  $600^\circ\text{C}$ , and  $700^\circ\text{C}$ , respectively.

To verify the micro-structure of  $\text{Co}_3\text{O}_4$ , the TEM image of  $\text{Co}_3\text{O}_4$  nanoparticles calcined at  $500^\circ\text{C}$  is shown in Fig. 3. From Fig. 3(a), it can be seen that  $\text{Co}_3\text{O}_4$  nanoparticles are uniformly dispersed and their size is less than 20 nm. As shown in Fig. 3(b), the lattice fringes of  $\text{Co}_3\text{O}_4$  can be observed clearly. The fringes with spacing of 0.46 nm correspond to (111) lattice plane (JCPDS42-1467) of the cubic  $\text{Co}_3\text{O}_4$ , suggesting  $\text{Co}_3\text{O}_4$  nanoparticles exhibit good crystallinity.

The UV-Vis spectra of  $\text{Co}_3\text{O}_4$  nanoparticles are shown in Fig. 4. As can be seen from Fig. 4, there are two broad peaks in the wavelength range of 300 to 450 nm and 600 to 750 nm. The first peak can be assigned to  $\text{O}^{2-}$  to  $\text{Co}^{2+}$  charge transfer, and the second one can be assigned to  $\text{O}^{2-}$  to  $\text{Co}^{3+}$  charge transfer.<sup>30</sup> The peak intensity of  $\text{Co}_3\text{O}_4$  nanoparticles calcined at  $500^\circ\text{C}$  is the highest, which indicates that  $\text{Co}_3\text{O}_4$  nanoparticles calcined at  $500^\circ\text{C}$  can absorb more light. When the temperature is higher than  $500^\circ\text{C}$ , the peak intensity decreases gradually. As discussed by XRD, the size of  $\text{Co}_3\text{O}_4$  nanoparticles calcined at  $500^\circ\text{C}$  is the smallest, and the nanoparticles size increases with the increase of temperature. This suggests that the calcination temperature not only affects the grain size but also the light absorption.

Figure 5 shows the amount of the hydrogen and oxygen evolution under visible irradiation over  $\text{Co}_3\text{O}_4$  calcined at  $450^\circ\text{C}$  and  $500^\circ\text{C}$  as the function of the irradiation time. From Fig. 5(a), the evolution of the hydrogen is  $247.1 \mu\text{molg}^{-1}$  and that of the oxygen is  $109.5 \mu\text{molg}^{-1}$  for  $\text{Co}_3\text{O}_4$  photocatalyst calcined at  $450^\circ\text{C}$  in 5 h without use of any cocatalyst and sacrificial agent. Moreover, the ratio of the hydrogen to the oxygen is almost 2:1.  $\text{Co}_3\text{O}_4$  calcined at  $500^\circ\text{C}$  also showed the same trend. For overall water splitting, the amount of the hydrogen evolution is  $259.4 \mu\text{molg}^{-1}$  and that of the oxygen is  $135.7 \mu\text{molg}^{-1}$  in 5 h using  $\text{Co}_3\text{O}_4$  calcined at  $500^\circ\text{C}$

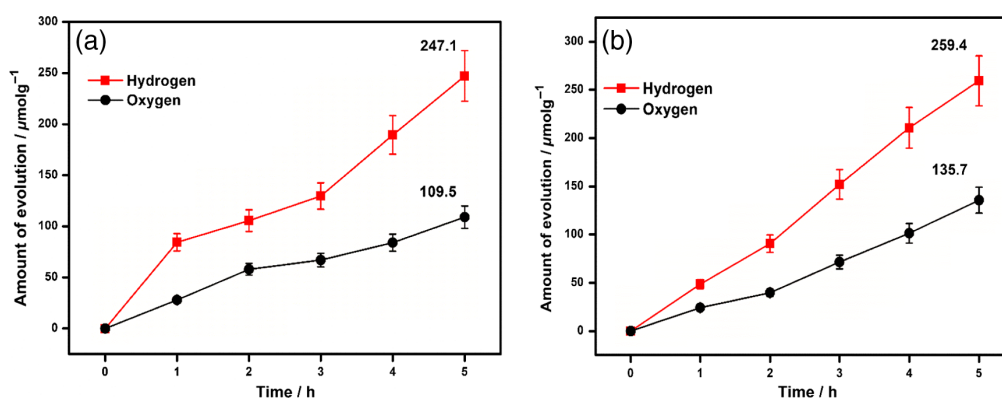


**Fig. 5** Reaction time courses of the hydrogen and the oxygen evolution under visible irradiation over  $\text{Co}_3\text{O}_4$  calcined at different temperatures: (a) 450°C and (b) 500°C.

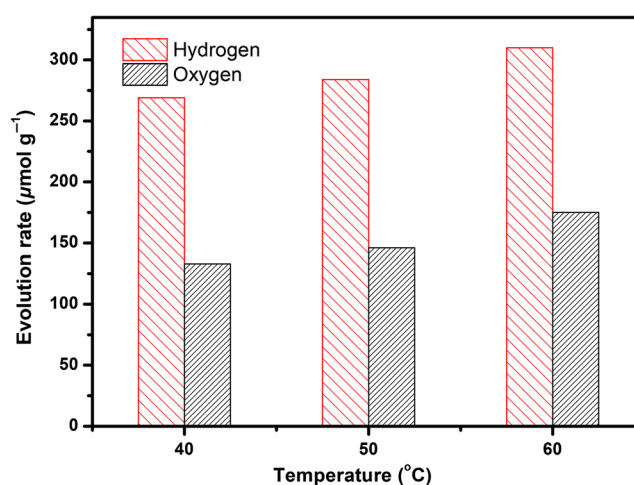


**Fig. 6** Amount of the hydrogen and the oxygen evolution under visible irradiation in 5 h over  $\text{Co}_3\text{O}_4$  calcined at 500°C as the function of the ambient temperature.

as shown in Fig. 5(b). Obviously,  $\text{Co}_3\text{O}_4$  photocatalyst calcined at 500°C shows the better photocatalytic activity than that of  $\text{Co}_3\text{O}_4$  calcined at 450°C and is chosen for further photocatalytic experiments by controlling the ambient temperature.

To study the effect of the ambient temperature on the photocatalytic process, the reaction temperature was controlled at 40°C, 50°C, and 60°C, and the results about the amount of the hydrogen and the oxygen evolution are shown in Fig. 6. With the increase of temperature, the evolution of hydrogen and oxygen also increases. The increase of the evolution may be due to the increase in kinetics of the reaction. The increase of temperature effect may increase the mobility of carriers. These charge carriers then move on to the surface with less recombination rate and react fast to produce hydrogen and oxygen. As shown in Fig. 6, the amount of hydrogen at 40°C, 50°C, and 60°C is 268.9, 284.6, and 310.7  $\mu\text{mol g}^{-1}$ , respectively, while the amount of oxygen is 133.1, 146.4, and 175.3  $\mu\text{mol g}^{-1}$ , respectively. Obviously, the ratio of the hydrogen to oxygen is near 2:1 in all experiments, which means that  $\text{Co}_3\text{O}_4$  photocatalyst can completely split pure water without using any cocatalyst and sacrificial agent.

The photocatalytic stability of  $\text{Co}_3\text{O}_4$  nanoparticles was evaluated under visible light irradiation at room temperature for 12 h. The experiment was done in three cycles. After 4 h of each cycle, the photocatalyst was recovered by centrifugation and drying and used in the next cycle. Figure 7 shows the stability performance of  $\text{Co}_3\text{O}_4$  over three cycles. It can be seen from Fig. 7 that the hydrogen and the oxygen evolution of the latter cycle is only slightly lower than that of the previous cycle, and the reduction rate is less than 9%, which suggests that the  $\text{Co}_3\text{O}_4$  for overall water splitting is stable.

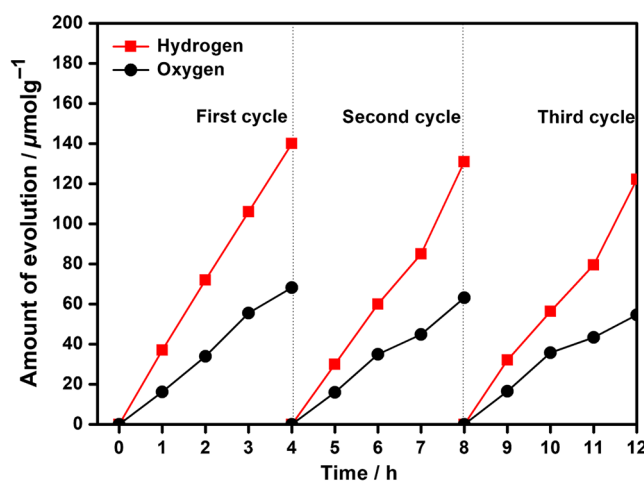


**Fig. 7** Reaction time courses of the hydrogen and the oxygen evolution under the visible irradiation over  $\text{Co}_3\text{O}_4$  calcined at  $500^\circ\text{C}$  at room temperature.

## 4 Conclusion

Through this environmentally friendly and inexpensive method,  $\text{Co}_3\text{O}_4$  nanoparticles were successfully synthesized using the bread fungus as green materials. These nanoparticles calcined at  $500^\circ\text{C}$  had the smallest grain size, the uniform distribution, and the best light absorption. Furthermore,  $\text{Co}_3\text{O}_4$  nanoparticles were used as a photocatalyst for overall water splitting under visible light irradiation without any cocatalyst and sacrificial agent. The evolution rates of the hydrogen and the oxygen increased by increasing the photocatalytic temperature, and the ratio of the hydrogen and the oxygen is close to 2:1. In addition,  $\text{Co}_3\text{O}_4$  photocatalyst had a good stability. Especially,  $\text{Co}_3\text{O}_4$  calcined at  $500^\circ\text{C}$  showed a good photocatalytic performance. Within 5 h, the amount of hydrogen and oxygen is  $259.4$  and  $135.7 \mu\text{mol g}^{-1}$ , respectively. Therefore, the green synthesis of cobalt oxide is a promising method for overall water splitting.

## Acknowledgments

This work was supported by the Natural Science Foundation of China (Nos. 21878242 and 21828802), Fundamental Research Funds for the Central Universities of China (No. xzd012020045), and Key Research and Development Projects of Shaanxi Province (Nos. 2018GY097 and 2018SF383).

## References

1. X. J. Guan et al., "Making of an industry-friendly artificial photosynthesis device," *ACS Energy Lett.* **3**(9), 2230–2231 (2018).
2. X. H. Liu et al., "In situ synthesis of ultrafine metallic  $\text{MoO}_2$ /carbon nitride nanosheets for efficient photocatalytic hydrogen generation: a prominent cocatalytic effect," *Catal. Sci. Technol.* **10**, 4053–4060 (2020).
3. T. Takata et al., "Photocatalytic water splitting with a quantum efficiency of almost unity," *Nature* **581**, 411–414 (2020).
4. X. J. Guan et al., "Efficient unassisted overall photocatalytic seawater splitting on GaN-based nanowire arrays," *J. Phys. Chem. C* **122**(25), 13797–13802 (2018).
5. Q. Wang et al., "Particulate photocatalysts for light-driven water splitting: mechanisms, challenges, and design strategies," *Chem. Rev.* **120**, 919–985 (2020).
6. S. Cao et al., "Emerging photocatalysts for hydrogen evolution," *Trends Chem.* **2**, 57–70 (2020).
7. Z. Hu et al., "An elemental phosphorus photocatalyst with a record high hydrogen evolution efficiency," *Angew. Chem. Int. Ed.* **55**, 9580–9585 (2016).

8. C. M. Wolff et al., "All-in-one visible-light-driven water splitting by combining nanoparticulate and molecular co-catalysts on CdS nanorods," *Nat. Energy* **3**, 862–869 (2018).
9. M. A. Sayed et al., "Photocatalytic hydrogen generation from raw water using zeolite/polyaniline @Ni<sub>2</sub>O<sub>3</sub> nanocomposite as a novel photo-electrode," *Energy* **187**, 115943 (2019).
10. D. Y. Chen et al., "Construction of Ni-doped SnO<sub>2</sub>-SnS<sub>2</sub> heterojunctions with synergistic effect for enhanced photodegradation activity," *J. Hazard. Mater.* **368**, 204–213 (2019).
11. Z. Wang et al., "Phosphorus-doped Co<sub>3</sub>O<sub>4</sub> nanowire array: a highly efficient bifunctional electrocatalyst for overall water splitting," *ACS Catal.* **8**(3), 2236–2241 (2018).
12. M. Mishra and D.-M. Chun, " $\alpha$ -Fe<sub>2</sub>O<sub>3</sub> as a photocatalytic material: a review," *Appl. Catal. A: Gen.* **498** (5), 126–141 (2015).
13. Z. Wang et al., "Identifying copper vacancies and their role in the CuO based photocathode for water splitting," *Angew. Chem. Int. Ed.* **58**, 17604–17609 (2019).
14. Z. W. Chen et al., "Recent advances in tin dioxide materials: some developments in thin films, nanowires, and nanorods," *Chem. Rev.* **114**, 7442–7486 (2014).
15. R. T. Huang et al., "Environmentally benign synthesis of Co<sub>3</sub>O<sub>4</sub>-SnO<sub>2</sub> heteronanorods with efficient photocatalytic performance activated by visible light," *J. Colloid. Interf. Sci.* **542**, 460–468 (2019).
16. A. Jelinska et al., "Enhanced photocatalytic waters splitting on very thin WO<sub>3</sub> films activated by high-temperature annealing," *ACS Catal.* **8**(11), 10573–10580 (2018).
17. S. Farhadi, K. Pourzare, and S. Sadeghinejad, "Simple preparation of ferromagnetic Co<sub>3</sub>O<sub>4</sub> nanoparticles by thermal dissociation of the [Co<sup>II</sup>(NH<sub>3</sub>)<sub>6</sub>](NO<sub>3</sub>)<sub>2</sub> complex at low temperature," *J. Nanostruct. Chem.* **3**(16), 1–7 (2013).
18. G. Kwak et al., "Preparation method of Co<sub>3</sub>O<sub>4</sub> nanoparticles using ordered mesoporous carbons as a template and their application for Fischer–Tropsch synthesis," *J. Phys. Chem. C* **117**(4), 1773–1779 (2013).
19. H.-P. Cong and S.-H. Yu, "Shape control of cobalt carbonate particles by a hydrothermal process in a mixed solvent: an efficient precursor to nanoporous cobalt oxide architectures and their sensing property," *Cryst. Growth Des.* **9**(1), 210–217 (2009).
20. S. Q. Chen and Y. Wang, "Microwave-assisted synthesis of a Co<sub>3</sub>O<sub>4</sub>-graphene sheet-on-sheet nanocomposite as a superior anode material for Li-ion batteries," *J. Mater. Chem.* **20**(43), 9735–9739 (2010).
21. R. C. Ambare, S. R. Bharadwaj, and B. J. Lokhande, "Non-aqueous route spray pyrolyzed Ru:Co<sub>3</sub>O<sub>4</sub> thin electrodes for supercapacitor application," *Appl. Surf. Sci.* **349**, 887–896 (2015).
22. J. K. Sharma et al., "Green synthesis of Co<sub>3</sub>O<sub>4</sub> nanoparticles and their applications in thermal decomposition of ammonium perchlorate and dye-sensitized solar cells," *Mater. Sci. Eng. B* **193**, 181–188 (2015).
23. N. O. M. Dewi et al., "Green synthesis of Co<sub>3</sub>O<sub>4</sub> nanoparticles using *Euphorbia heterophylla* L. leaves extract: characterization and photocatalytic activity," *IOP Conf. Ser.: Mater. Sci. Eng.* **509**, 012105 (2019).
24. R. Sathyavathi, M. Krishna, and D.N. Rao, "Biosynthesis of silver nanoparticles using *Moringa oleifera* leaf extract and its application to optical limiting," *J. Nanosci. Nanotechnol.* **11**, 2031–2035 (2011).
25. J. Osuntokun, D. C. Onwudiwe, and E. E. Ebenso, "Green synthesis of ZnO nanoparticles using aqueous *Brassica oleracea* L. var. italica and the photocatalytic activity," *Green Chem. Lett. Rev.* **12**(4), 444–457 (2019).
26. M. R. AbuKhadra et al., "Enhanced photocatalytic degradation of acephate pesticide over MCM-41/Co<sub>3</sub>O<sub>4</sub> nanocomposite synthesized from rice husk silica gel and peach leaves," *J. Hazard. Mater.* **389**, 122129 (2020).
27. M.A. Salam et al., "Insight into the adsorption and photocatalytic behaviors of an organobentonite/Co<sub>3</sub>O<sub>4</sub> green nanocomposite for malachite green synthetic dye and Cr(VI) metal ions: application and mechanisms," *ACS Omega* **5**, 2766–2778 (2020).
28. J. Chen et al., "An ultrafast supercapacitor built by Co<sub>3</sub>O<sub>4</sub> with tertiary hierarchical architecture," *Vacuum* **174**, 109219 (2020).

29. T. Chang et al., "Post-plasma-catalytic removal of toluene using  $\text{MnO}_2\text{-Co}_3\text{O}_4$  catalysts and their synergistic mechanism," *Chem. Eng. J.* **348**, 15–25 (2018).
30. M. K. Uddin and U. Baig, "Synthesis of  $\text{Co}_3\text{O}_4$  nanoparticles and their performance towards methyl orange dye removal: characterization, adsorption and response surface methodology," *J. Clean. Prod.* **211**, 1141–1153 (2019).

**Qing-Yun Chen** is a professor in State Key Laboratory of Multiphase Flow in Power Engineering, Xi'an Jiaotong University. She obtained her PhD from Nara Women's University of Japan in 2007. She joined Xi'an Jiaotong University in 2008 and her research interests have focused on photocatalysis for water splitting.

Biographies of the other authors are not available.